

# TFMi™: Using Intermodal Analysis to Improve TFM Imaging

Paul Holloway<sup>1</sup> and Ed Ginzel<sup>2</sup>

<sup>1</sup>Holloway NDT & Engineering Inc, Georgetown, Ontario, Canada  
e-mail: [paul@hollowayndt.com](mailto:paul@hollowayndt.com), website [www.hollowayndt.com](http://www.hollowayndt.com)

<sup>2</sup> Materials Research Institute, Waterloo, Ontario, Canada  
e-mail: [eginzel@mri.on.ca](mailto:eginzel@mri.on.ca)

2021.05.03

## Abstract

In recent years, phased array ultrasonic inspections have incorporated a variety of total focussing methods (TFM) to process data collected from full matrix capture techniques. The results are images that can greatly assist in characterization and sizing of indications. Codes have been written to standardise the techniques [1,2,3]. Because these codes use a qualification process, they specify that the selection of propagation modes used in the TFM construction are identified. Experience has demonstrated that not all combinations of paths are effective at detecting indications in TFM. The user is left to determine which propagation mode produces the best result. In this paper we illustrate how the process can be improved in both detection and reliability by simultaneously processing multiple modes in combination.

**Keywords:** ultrasonic, phased array, FMC, TFM, total focussing method

## 1. Introduction

Total Focussing Method (TFM) is a term given to the mathematical processing of waveforms collected by a phased array data acquisition process to provide an image of a volume under inspection.

Acquisition techniques can be one of several options:

- Full Matrix Capture (FMC)
- Half Matrix Capture (HMC)
- Sparse Matrix Capture
- Plane Wave Imaging (PWI)
- Synthetic Aperture Focussing Technique (SAFT)

The most common approach is FMC, where each element of a phased array probe is used as an independent transmitter and receiver. An illustration of the transmitting and receiving operations using a small 4-element transducer is shown in Figure 1. The echo from each transmitted pulse is



recorded as a separate A-scan for each receiving element. As a result, the simple 4-element FMC dataset would result in 16 A-scans (blue arrows).

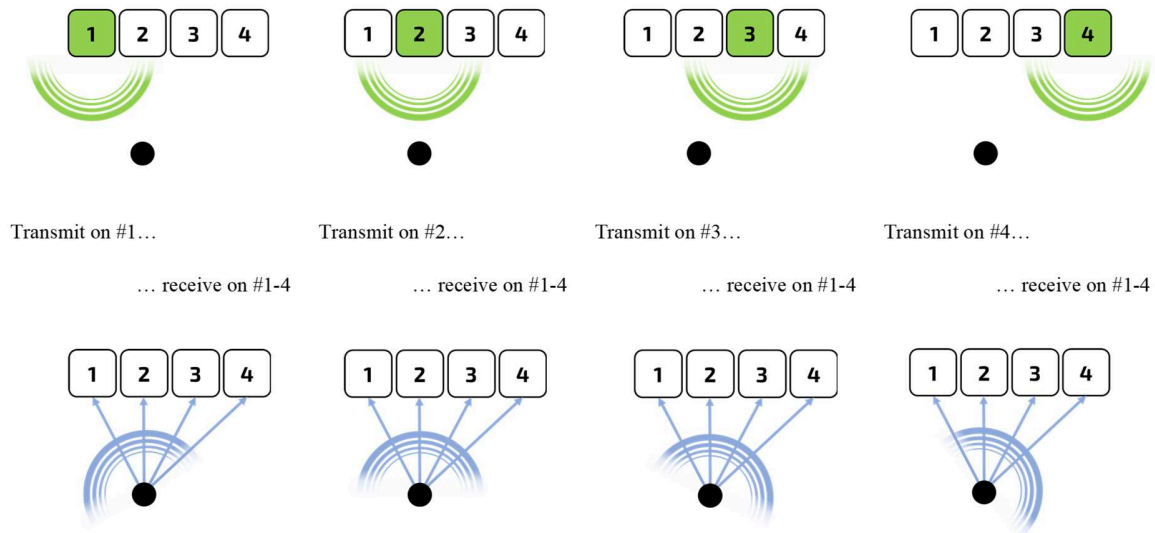


**Figure 1: Simplified 4-element full matrix capture**

For a transducer of  $n$  elements, it is possible to capture up to a maximum of  $n^2$  A-scans with a full matrix capture approach. For a 32-element transducer, an FMC dataset would produce  $(32)^2$  or 1,024 A-scans, and a 64-element transducer would produce 4,096 A-scans. These figures represent the number of A-scans *per scan frame*, or scan position. A small weld sample 300mm long scanned in 1mm scan increments using 64-elements would require over 1.2 million A-scans. Raw FMC datasets can become incredibly large and do not present useful images alone without further processing. Capture techniques such as sparse matrix capture (SMC) and half matrix capture (HMC) use fewer elements or store fewer A-scans which help in acquisition speed. However, FMC datasets provide the most data and possibilities for imaging algorithms.

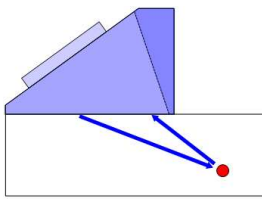
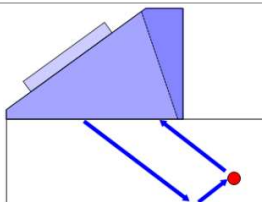
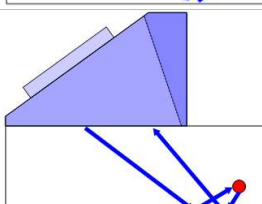
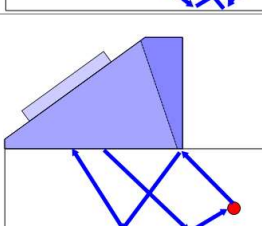
Having acquired the waveform data with one of the acquisition techniques, there are several ways to process the data to obtain an image that can be useful. The TFM algorithm uses a process of delay and summing of waveforms. Each received waveform can be calculated for its point of origin in the region of interest (ROI), and signals from boundaries in the same location will add as coherent sources. This results in larger amplitude summations where flaws or other discontinuities are located. When plotted, signals are reconstructed as points of higher amplitude when there is constructive interference from echoes received at each element. TFM can be applied as a processing option regardless of the type of acquisition (FMC, HMC, PWI, etc.). TFM can be used to synthetically generate a focus everywhere in the ROI by applying different virtual focal laws to the collected A-Scans.

The same set of FMC data can be used multiple times using different combinations of reconstruction parameters. Critical in the success of the TFM is the selection of the propagation

mode that could occur for each pixel in the ROI. Flaws can be imaged from multiple directions when boundary reflections are included in the path from transmitter to receiver. This applies to both reflected and diffracted signals. Coherent signals in a pixel region arriving from multiple modes and directions will improve results by increased reliability of detecting flaws and reduced occurrence of artifacts [4,5].

The following table is an overview of the primary propagation modes used with TFM for inspection of carbon steel welds using a refracting wedge:

**Table 1: TFM Propagation Modes for General Weld Inspection**

Imaging Path	Nomenclature	Description
	T-T (2T)	Two paths: 1. Transducer to discontinuity 2. Discontinuity back to transducer
	TTT (3T)	Three paths: 1. Transducer to backwall 2. Backwall to discontinuity 3. Discontinuity back to transducer  <i>(or reverse, i.e., to discontinuity first, then backwall)</i>
	TT-TT (4T)	Four paths: 1. Transducer to backwall 2. Backwall to discontinuity 3. Discontinuity to backwall 4. Backwall to transducer
	TTTTT (5T)	Five paths: 1. Transducer to backwall 2. Backwall to discontinuity 3. Discontinuity to front wall 4. Front wall to backwall 5. Backwall to transducer  <i>(or any other combination of 5 paths)</i>

ISO [3] guidance states that in general, planar flaws are best detected when the imaging paths have an incident angle and reflected angle on the flaw that is:

- a) (about) perpendicular to the discontinuity orientation;
- b) (about) symmetric to the normal direction of the discontinuity, or
- c) according to Snell's law if mode-conversion occurs at the discontinuity.

The combination of paths and modes used to image a volume in an ROI becomes a challenge for the operator qualifying a procedure using TFM. The selection of the right mode of propagation often requires some foresight into the nature of the flaw under investigation (i.e. “we need to know what we’re looking for before we start looking for it”). If the wrong mode is selected, the flaw may be completely overlooked (porosity detected with PA sectorial and TFM TT mode, but missed with TFM LTL mode, Figure 2 to Figure 4). Even if the recommended mode is selected (e.g., 3T for a root connected crack), the image may fail to accurately represent the flaw if the reflecting faces are tilted.

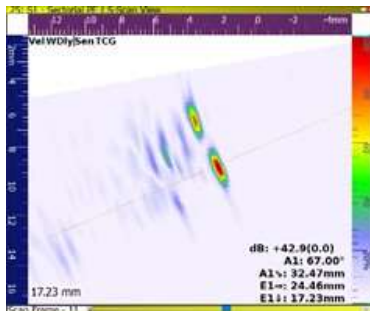


Figure 2: PAUT sectorial

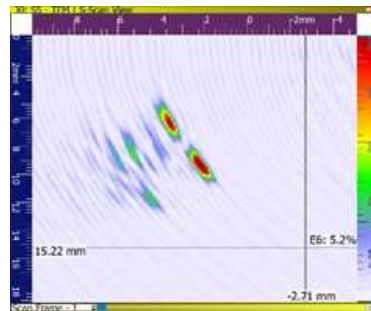


Figure 3: TFM TT mode

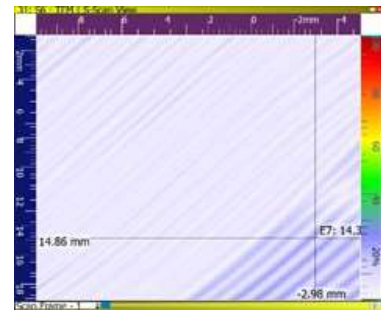


Figure 4: TFM LTL-mode

In this paper we illustrate a new approach called TFMi<sup>TM</sup> that combines multiple, standard TFM propagation mode images via multiplication of pixel values along with the introduction of a non-linear amplitude factor. The multiplication approach not only greatly enhances signal-to-noise ratio (SNR), but also improves reliability of detection and flaw characterization.

## 2. Basis of Intermodal Analysis

The basic TFMi<sup>TM</sup> image is generated by combining the images of a selected number of standard TFM propagation modes by multiplication. Amplitude values at each pixel co-ordinate are a product of the corresponding pixel values of each component mode. *Coherent signals are amplified*, thus high amplitude responses in two or more modes are enhanced. Similarly, *incoherent signals are suppressed*, which greatly reduces background noise. Any combination of modes may be used in TFMi<sup>TM</sup>. This paper focuses on the results from the basic 2T, 3T, 4T and 5T combinations.

As an example, a TFMi<sup>TM</sup> image of a porosity cluster using a combination of the 2T, 3T, 4T and 5T modes would be generated as follows:

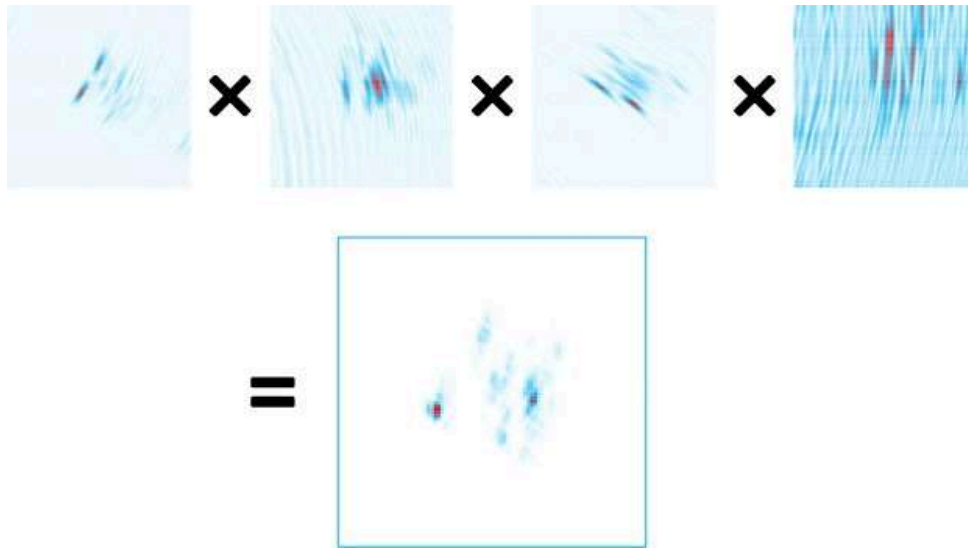


**Figure 5: TFMi™ basic image, porosity sample (2T x 3T x 4T x 5T)**

As an additional step, a non-linear amplification filter may be applied to reveal low amplitude details while retaining the low noise floor. A comparison between a final TFMi™ image and an image generated with simple intermodal addition is shown in Figure 6 and Figure 7. This additional filtering process may not always be required.

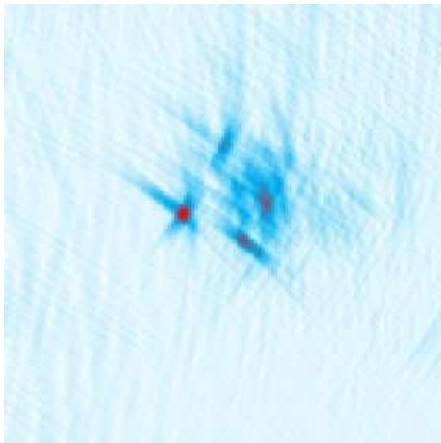


**Figure 6: Intermodal addition**

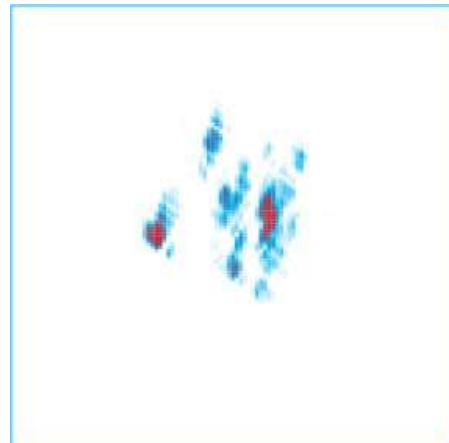


**Figure 7: TFMi™ image after application of a non-linear amplification filter**

### 3. Test Programme

To demonstrate the performance of TFMi™ on real flaws, a basic FMC was configured on several flawed specimen samples fabricated by reputable manufacturers used in the NDT industry, plus one additional specimen with an artificial 3-segment crack.

All testing was performed with transducers mated to PAUT shear wave wedges to simulate field conditions during weld inspection.

Instrumentation used was:

- Sonatest Veo+ 32:128 outfitted with development software
- Olympus 5L32-A31 transducer (5MHz, 32-elements, 0.6mm pitch)
  - Full 32-elements used in FMC acquisition
  - Mated to a 55-degree shear wave wedge
- Vermon-NDT A10L64-12 transducer (10MHz, 64-elements, 0.3mm pitch)
  - Tests performed using 32 and 64-elements in FMC acquisition
  - Mated to a 55-degree shear wave wedge

### 3.1. Artificial crack

To test the capabilities on crack-like reflectors, a 25mm thick steel block was manufactured with three crack features varying in complexity from 1 to 3-segments (Figure 8). The vertical height of each segment was 5mm, making the maximum height of the 3-segment crack 15mm.

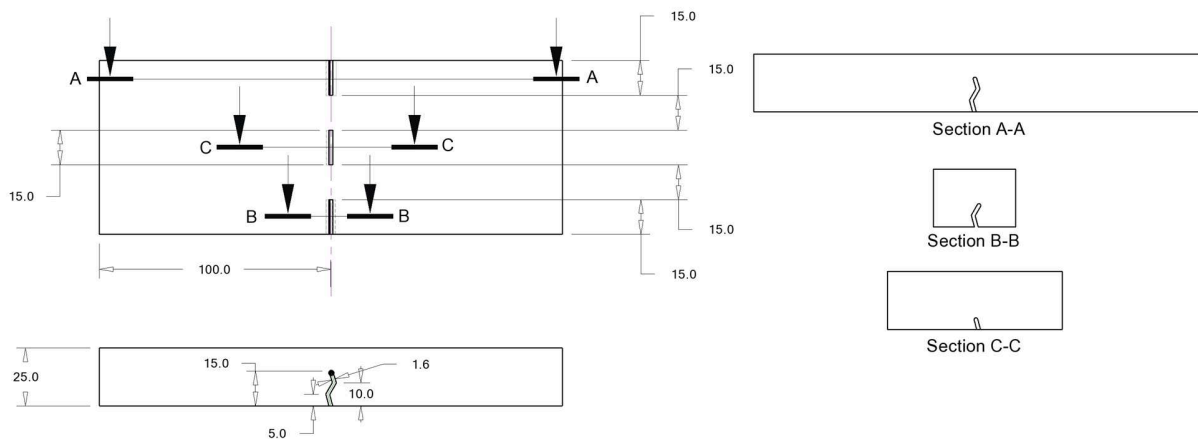


**Figure 8: Machined 3-segment crack feature**

The crack cross-sections are shown in the section views. Each section was scanned from both directions (probe on left/right) with PA sectorial, 2T through 5T propagation modes, and TFMi<sup>TM</sup>. The probes were positioned at an offset distance typical for a double-V weld to represent inspection conditions (Figure 9).

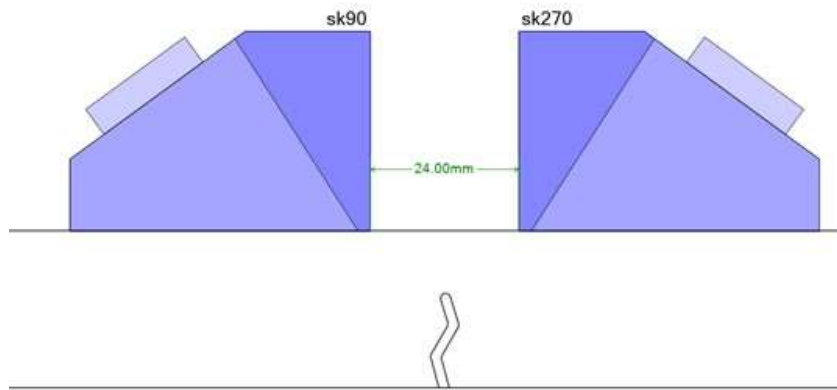


**Figure 9: 3-segment machined crack probe positions**

Neither the PA sectorial nor any of the regular TFM modes provide much information on the complex shape of the feature. The TFMi™ group images the crack clearly from both skews with extremely high signal-to-noise ratio in comparison with the individual modes (Figure 10, Figure 11).

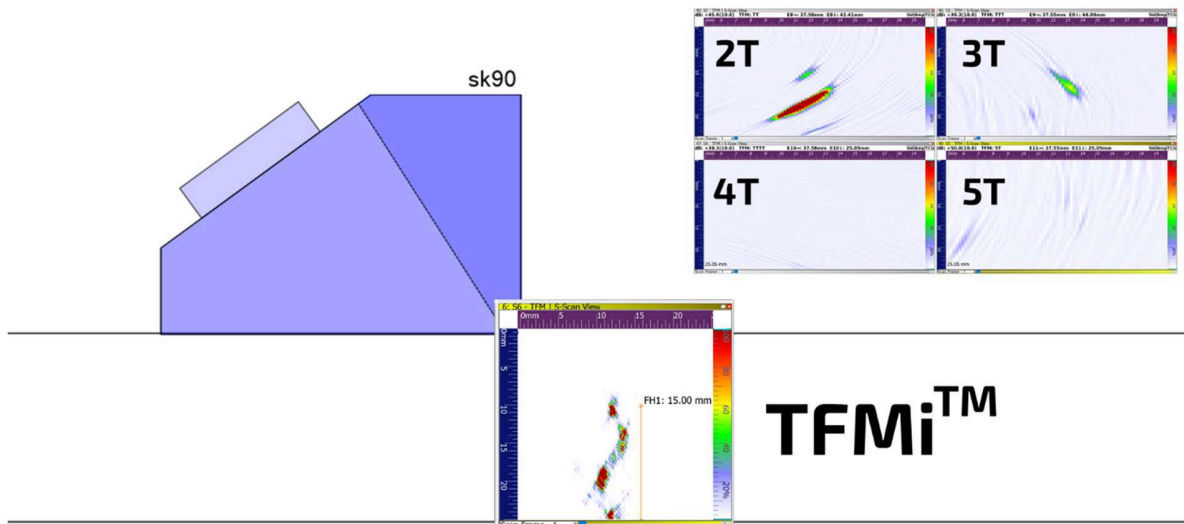


**Figure 10: Skew 90, Section A-A**

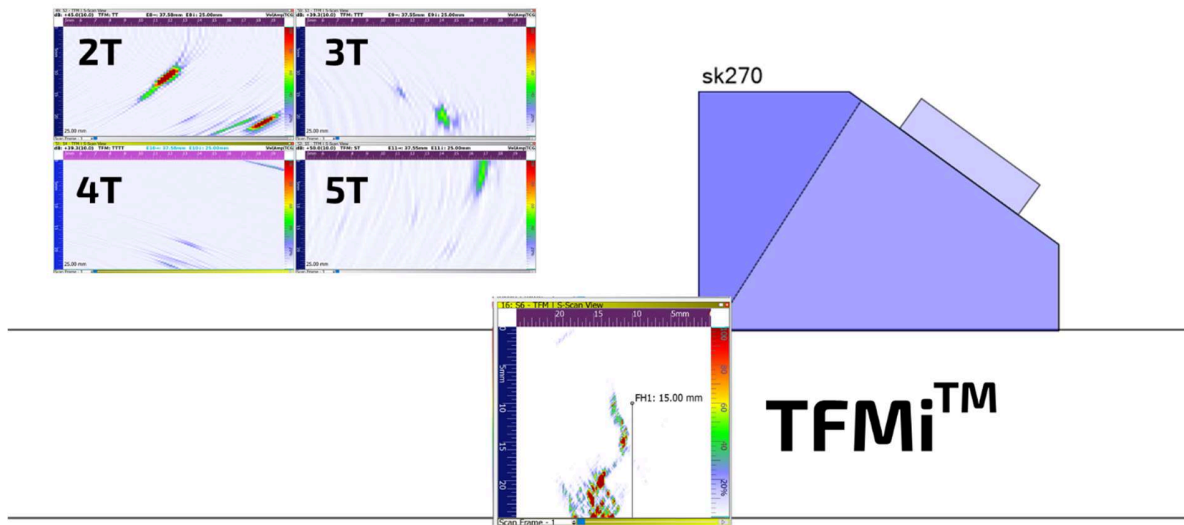


Figure 11: Skew 270, Section A-A

The images from the smaller sections B-B and C-C are shown in Figure 12. Depth cursors are provided in each image to validate sizing measurements. The full height in Section A-A (15mm, above) and Section C-C (5mm, below) are sized accurately from both sides. Section B-B (10mm, below) from the Skew 90 orientation was undersized by approximately 2-3mm, likely due to the wide milling bit used to form the crack and the diminished tip diffraction echo.

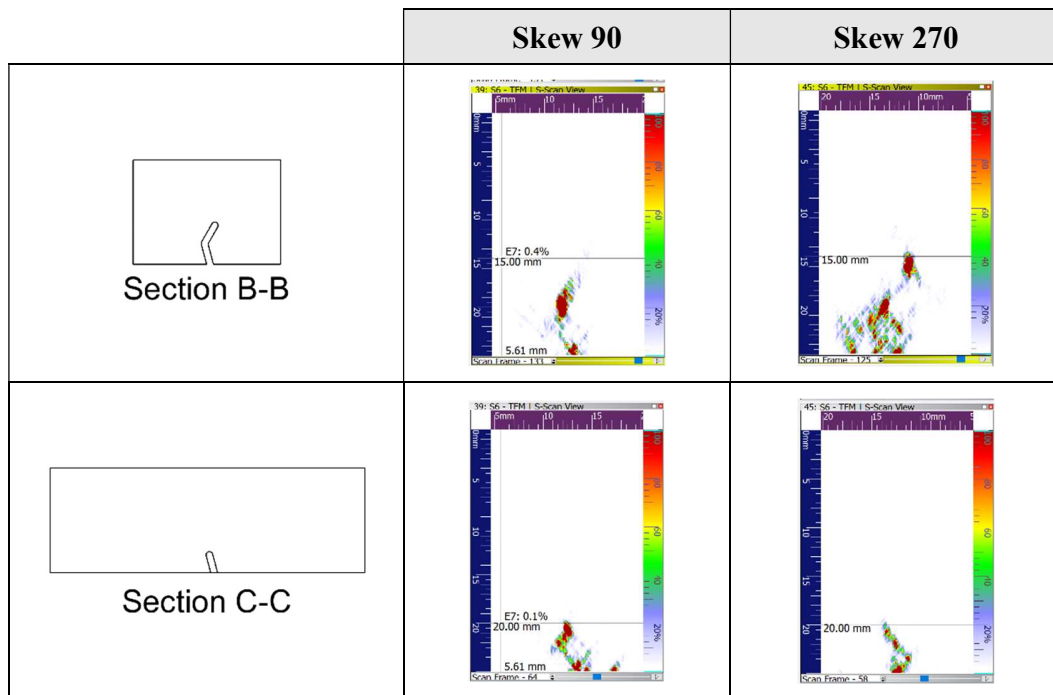


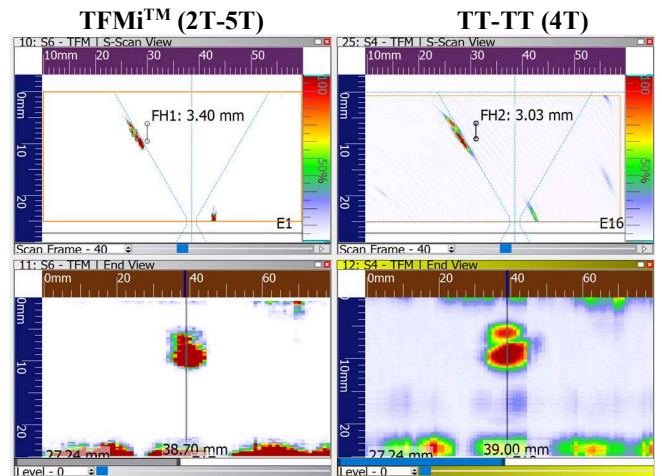
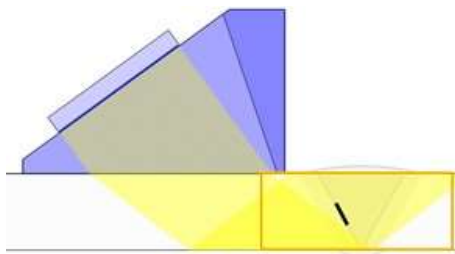


Figure 12: 3-segment machined crack, TFMi™ images on Sections B-B and C-C

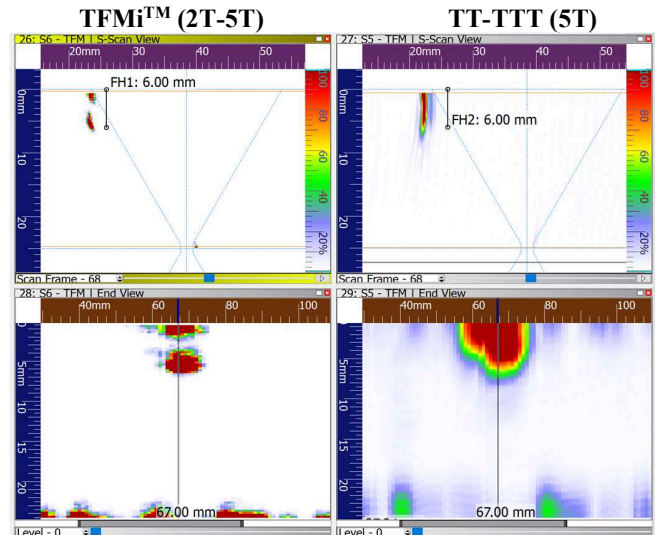
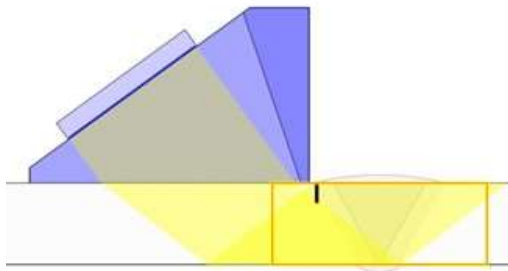
### 3.2. Real Weld Flaws

The following shows the comparison between TFMi™ and standard TFM modes on a variety of realistic weld flaws. The projected views shown below the TFM frames are useful for displaying the length (horizontal axis) and height (vertical axis) of reflectors.

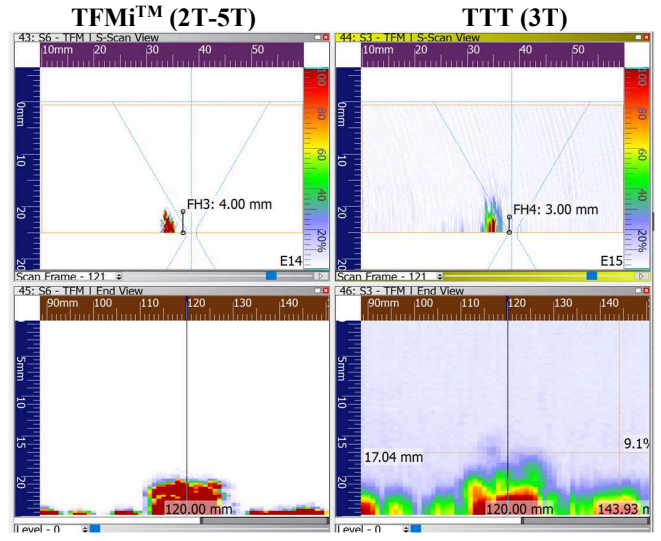
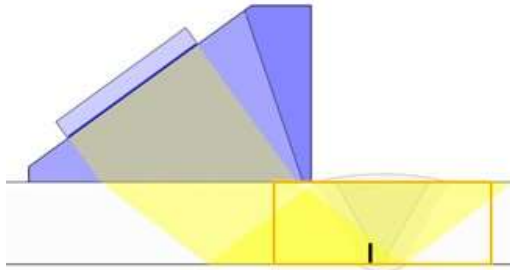
#1 - Lack of Sidewall Fusion



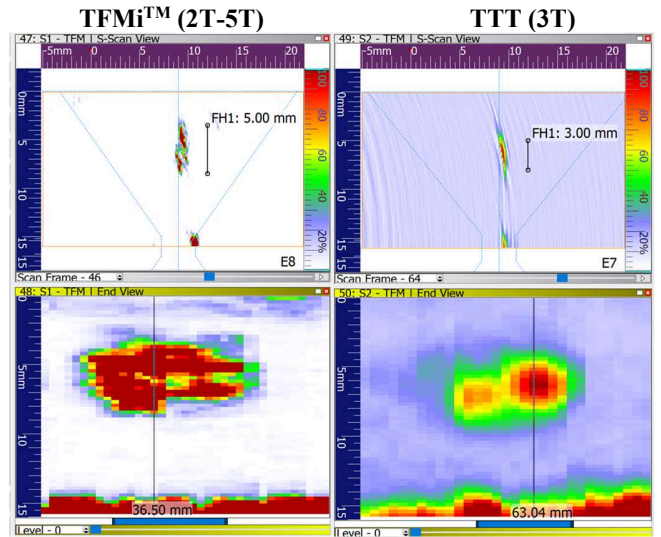
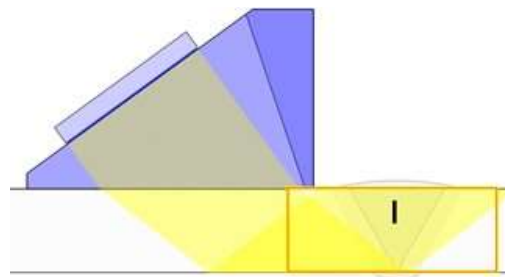
#2 - Toe Crack



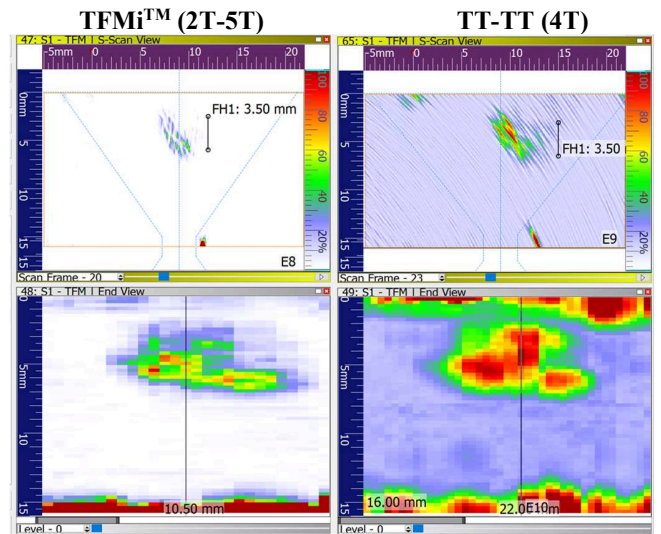
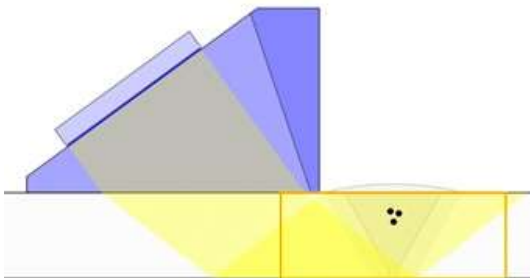
#3 - Root Crack



#4 - Centreline Crack



#5 - Porosity



The table below summarizes the height sizing performed with TFMi<sup>TM</sup> compared to other techniques:

**Table 2: Flaw Height Size Summary**

	PAUT (tip echo)	TOFD	TFM	(TFMi <sup>TM</sup> )
#1 Lack of fusion	3.3 mm	4.2 mm	3.6 mm (TT-TT)	3.8 mm
#2 Toe crack	6.7 mm	6.5 mm	6.3 mm (5T)	6.0 mm
#3 Root crack	4.0 mm	5.1 mm	5.5 mm (3T)	4.4 mm
#4 Centreline crack	4.0 mm	N/A	4.0 mm (3T)	4.0 mm
#5 Porosity	4.5 mm	N/A	4.8 mm (4T)	4.9 mm

#### 4. Discussion

As noted in the introduction, TFMi<sup>TM</sup> has the potential to improve reliability of detection, enhance the detail of the imaged flaw for sizing and reduce the occurrence of unwanted image artifacts. In some cases, standard TFM may provide no evidence of a flaw (Figure 13 vs. Figure 14 below).

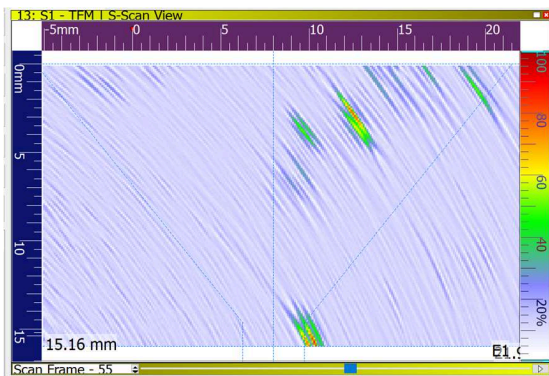


**Figure 13: Centreline crack, TT-TT mode**

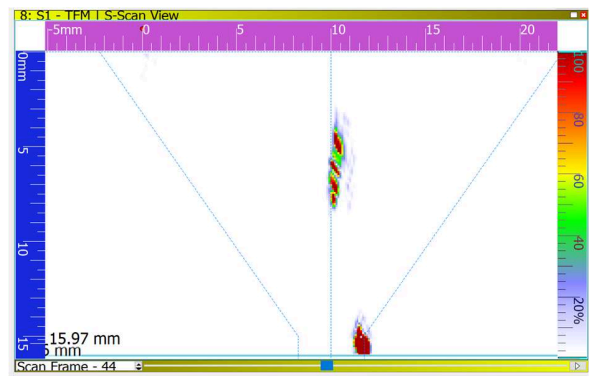


**Figure 14: Centreline crack, TFMi<sup>TM</sup>**

Note that some combinations of TFM produce artifacts from mode conversion (false positives). Intermode combination with TFMi<sup>TM</sup> can be used to suppress these artifacts.

Multiplication of modes with TFMi<sup>TM</sup> greatly increases the signal-to-noise ratio (SNR) of the image. All images in this paper use the same colour palette with the same 0-100% range. The white background in the TFMi<sup>TM</sup> images represents pixel values of less than 1% range. SNR comparisons between standard TFM, intermode analysis by addition, and TFMi<sup>TM</sup> are shown in Figure 15 to Figure 17. Note the SNR values shown are a ratio of the maximum pixel value in the indication area compared to the maximum pixel value in an area away from the indication.

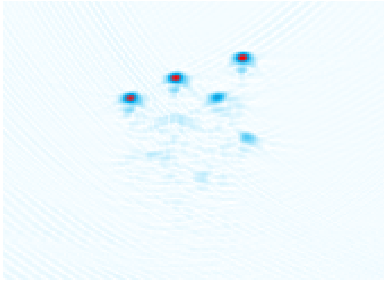


**Figure 15: TT mode**  
(SNR: 24.6)

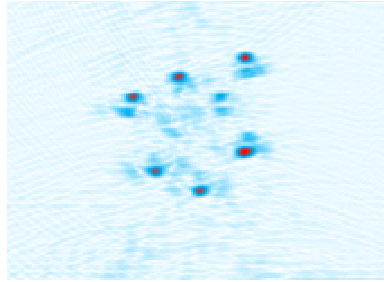


**Figure 16: Intermode addition**  
(SNR: 6.8)

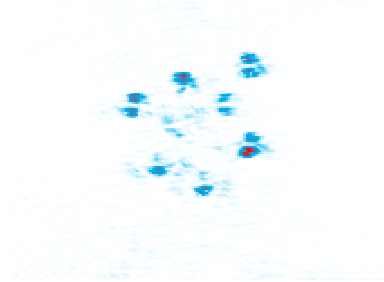


**Figure 17: TFMi™**  
(SNR: 86.9)

## 5. Conclusions

TFMi™ is a new approach to the basic TFM options. It provides improved detection and sizing, improved geometric fidelity and flaw characterization, and reduces the chance of false positives caused by artifact images. TFMi™ uses multiple propagation modes simultaneously to generate an image, and removes the guesswork required when limited to single modes.

Currently, TFMi™ is in development by Holloway NDT & Engineering Inc. and Sonatest. All images in this paper were generated using prototype software and/or post processed externally.

The use of intermodal analysis does not eliminate the need for examining mode responses individually. It is still recommended that procedures include use of PA sectorial and standard TFM propagation modes suited to characteristics of a known reflector. However, TFMi™ can reduce the number of iterations that might be used to optimise detection and can greatly enhance characterization and sizing of relevant indications.

### 5.1. Future Development

Possibilities for future development include:

- Pattern recognition between modes and a staging process for characterization to optimize mode combinations, which may include self comparisons, inclusion of an addition frame, and combining images from opposite skews
- 3D weld flaw modeling based on frame stacking
- Additional study on interaction with propagation modes using mode conversions (TTL, TLL, etc.)

## 6. Acknowledgements

We would like to express our thanks to Jonathan Lesage to detailed explanations of the various processes associated with the FMC/TFM techniques. We would also like to thank Philippe Rioux (Sonatest) and Steve Hudgins (Advanced Sound Solutions) for providing many of the samples used to illustrate TFMi™ in this paper.

## References

1. ASME Boiler and Pressure Vessel Code, Section V, American Society of Mechanical Engineers, Two Park Avenue • New York, NY • 10016 USA, 2019
2. ISO 23864, Non-destructive testing of welds — Ultrasonic testing — Use of automated total focusing technique (TFM) and related technologies. International Standards Organisation, Switzerland, 2021
3. ISO 23865, Non-destructive testing — Ultrasonic testing — General use of full matrix capture / total focusing technique (FMC/TFM) and related technologies. International Standards Organisation, Switzerland, 2021
4. Busse, L J, Collins, H D, and Doctor, S R. Review and discussion of the development of synthetic aperture focusing technique for ultrasonic testing (SAFT-UT). United States: N. p., 1984. Web. doi:10.2172/6977775.
5. Sy, K., Bredif, P., Iakovleva, E., Roy, O., & Lesselier, D. (2018). Development of methods for the analysis of multi-mode TFM images. *Journal of Physics: Conference Series*, 1017(1). <https://doi.org/10.1088/1742-6596/1017/1/012005>
6. N. Portzgen, D. Gisolf, D. Verschuur, Wave equation-based imaging of mode converted waves in ultrasonic NDI, with suppressed leakage from nonmode converted waves, *Ultrasonics, Ferroelectrics, and Frequency Control*, IEEE Transactions (2008)
7. E. Iakovleva, S. Chatillon, P. Bredif, S. Mahaut, Multi-mode TFM imaging with artifacts filtering using CIVA UT forwards models, *AIP Conference Proceedings*, Vol. 1581, 2014